On Deploying Bilinear Neural Network Method to Various Solutions of (3+1)-dimensional Potential Yu-Toda-Sasa-Fukuyama Equation

NGUYEN MINH TUAN, CHAU VAN VAN, NGUYEN HONG SON,
HUYNH TRONG THUA*, LE HA THANH
Faculty of Information Technology,
Posts and Telecommunications Institute of Technology,
Sai Gon ward, Ho Chi Minh city, 700000
VIETNAM

Corresponding Author

Abstract: This paper investigates the (3+1)-dimensional potential Yu-Toda-Sasa-Fukuyama (YTSF) equation using the Bilinear Neural Network Method (BNNM). This novel hybrid framework integrates Hirotas bilinear formalism with neural network modeling. By reformulating the YTSF equation into its bilinear form and embedding this structure into the BNNM architecture, multiple classes of exact analytical solutions are derived, including kink-type, periodic, and rational forms. The proposed method yields closed-form solutions that preserve mathematical rigor while improving computational efficiency for high-dimensional nonlinear evolution equations. The results demonstrate the effectiveness of the BNNM in generating diverse solution structures for the YTSF equation, providing potential applications in fluid dynamics, plasma physics, and other nonlinear physical models.

Key-Words: (3+1)-dimensional YTSF equation, Bilinear Neural Network Method (BNNM), Hirota bilinear form, nonlinear partial differential equations, exact solutions.

Received: May 24, 2025. Revised: July 17, 2025. Accepted: September 23, 2025. Published: May 22, 2026.

1 Introduction

Two-layer fluid systems are frequently used to describe nonlinear processes in fluid mechanics, thermodynamics, and the medical sciences. In this context, the generalized (3+1)-dimensional Yu-Toda-Sasa-Fukuyama (YTSF) equation has been used to study the interfacial wave dynamics of a two-layer liquid, [1]. The formulation of generalized bilinear differential equations based on Hirota operator analysis has been used to derive exact solutions for prospective YTSF-like equations with p=3 and p=5 using the generalized Hirota bilinear approach, [2]. Furthermore, the potential YTSF equation has been successfully solved using the extended complex method in conjunction with the (G'/G)-expansion methodology. This method improves our understanding of the structural features of the YTSF problem by producing a number of kinds of solutions, such as simply periodic functions, rational function solutions, and Weierstrass elliptic function solutions, [3].

Applications of the two-dimensional YTSF equation can also be found in plasma physics and other natural sciences. In addition to the power series expansion approach, which offers further explicit solutions for this model, Lie symmetry analysis has established exact analytical answers, [4], [5]. A new method called the homoclinic (heteroclinic) breather limit method (HBLM) has been proposed to capture rogue wave occurrences in nonlinear evolution equations (NEEs). This method produces a novel class of two-wave solutions, called rational breather wave solutions, which correspond to rogue waves, as shown by the (3+1)-dimensional YTSF equation, [6]. The following is the (3+1)-Dimensional Potential-YTSF Equation, [7]:

$$-4u_{xt}+u_{xxxz}+4u_xu_{xz}+2u_{xx}u_z+3u_{yy}=0, \quad (1.1)$$

The research of the YTSF equation in connection with interfacial waves in two-layer liquids and elastic quasiplane waves in lattices has advanced further. One- and two-bell soliton solutions have been generated using the Hirota technique, Bell polynomials, and symbolic computation, with Bőcklund transformations added, [7]. Furthermore, the nonlinear (3+1)-dimensional potential YTSF problem has yielded a wide range of explicit solutions, such as periodic wave solutions, classical solitons, and singular solitons, demonstrating the variety of wave phenomena this equation supports, [8].

Computational developments have transformed the study of nonlinear differential equations in recent years. Notably, strong frameworks for evaluating and resolving intricate nonlinear PDEs have been developed as a result of the development of the bilinear neural network method (BNNM) and softmax-based techniques, [9]. By fusing Hirota's bilinear formalism, a fundamental component of soliton theory, with the adaptive learning potential of neural networks, the BNNM represents a revolutionary fusion of integrable systems theory and contemporary machine learning. While improving computational efficiency, this hybrid technique maintains mathematical rigor.

The BNNM uses a training-free paradigm that incorporates the PDE structure directly into the network design, in contrast to conventional physics-informed neural networks that need a large amount of training data, [10]. Its ability to generate lump waves, rogue waves, and breather solutions has made it especially useful for high-dimensional problems, including (3+1)-dimensional breaking soliton equations. Additionally, the approach performs better when dealing with fractional nonlinear systems and nonlocal integrable equations than perturbation approaches and numerical discretization.

2 Fundamental Definitions

Significant advancements in computational frameworks for solving nonlinear differential equations can be seen in the bilinear neural network technique. They are essential for contemporary applied mathematics, physics, and engineering because they can represent intricate nonlinear behaviors, take into account limitations unique to a given situation, and function at scale. They provide a complimentary balance when used in tandem. Softmax ensures stability, normalization, and efficient selection of pertinent solutions, while BNNM offers a rich, adaptable representation of the solution manifold.

Definition 1. Hirota bilinear operator determined with the definition of D-operator is shown as the following expression, [9]:

$$D_t^m D_x^n f(t,x)\cdot g(t,x) = \frac{\partial^m}{\partial s^m}\frac{\partial^n}{\partial y^n} f(t+s,x+y)g(t-s,x-y)\bigg|_{s=0,y=0}, \quad m,n = 0,1,2,\ldots.$$

Using the differentiation of a product rule, the Leibniz rule could be compared by the transform shown as follows:

$$\frac{\partial^m}{\partial t^m}\frac{\partial^n}{\partial x^n} f(t,x)\cdot g(t,x) = \frac{\partial^m}{\partial s^m}\frac{\partial^n}{\partial y^n} f(t+s,x+y)g(t+s,x+y)\bigg|_{s=0,y=0}, \quad m,n = 0,1,2,\ldots.$$

Based on the bilinear neural network model shown in Fig. 1 (Appendix), the BNNM is constructed as the following:

Step 1: Transform Eq. (1.1) into its Hirota Bilinear Operator (HBO) form as described in Definition 1. Next, construct activation functions consistent with the BNNM using the test function. The general equation is shown as follows:

$$F\left(f, f_x, f_y, f_t, f_{xy}, f_{xt}, f_{yt}, f_{xyt}, \cdots\right) = 0, \tag{2.1}$$

where $f_x,\ f_y,\ f_t,\ f_{xx},\ f_{xt},\ f_{yt},\ \cdots$ demonstrate the derivative respect to $x, y, t, xx, xt, yt, \cdots$, respectively.

Step 2: Substitute activation function f from Eq. (3.5) to derive algebraic equations in terms of variables such as x, t, y, xy, xt, yt, $F(x,y,z,t), \cdots$ and others.

Step 3: Solve the resulting system of equations to determine the values of the coefficients of the test functions.

Step 4: Substitute the test functions back into Eq. (3.5) to construct the exact analytical solutions.

Step 5: Verify that the solutions u obtained satisfied Eq. (1.1) through direct substitution and validation.

3 Hirota Bilinear Form of YSTF equation

The original equation will be converted to Hirota's bilinear form in order to execute a bilinear neural network approach for the (2+1)-dimensional breaking soliton system (BSS) equation as follows:

Setting traveling $\xi = \varepsilon x + py + qt + rz$, Eq. (1.1) is transformed to

$$\left(-4q\varepsilon + 3p^2\right)u_{\xi\xi} + r\varepsilon^3 u_{\xi\xi\xi\xi} + 6r\varepsilon^2 u_\xi u_{\xi\xi} = 0, \tag{3.1}$$

By using $\theta = \frac{r}{-4q+3p^2}$, and $\varepsilon = 1$, Eq. (3.1) becomes

$$u_{\xi\xi} + \theta\left[u_{\xi\xi\xi\xi} + 6u_\xi u_{\xi\xi}\right] = 0, \tag{3.2}$$

Using Painleve analysis $u = 2w_\xi, w = \ln f$, we attain the equation as follows:

$$2w_{\xi\xi\xi} + \theta\left[2w_{\xi\xi\xi\xi\xi} + 24w_{\xi\xi}w_{\xi\xi\xi}\right] = 0, \tag{3.3}$$

Integrating on both sides and letting constant equals zero, we have

$$w_{\xi\xi}+\theta\left[w_{\xi\xi\xi\xi}+6w_{\xi\xi}^2\right]=0, \tag{3.4}$$

Using the Hirota bilinear form, we construct the bilinear form as follows:

$$\left[D_\xi^2+\theta D_\xi^4\right]f\cdot f=0, \tag{3.5}$$

where

$$D_\xi^2 f\cdot f=2\left(f_{\xi\xi}f-f_\xi^2\right),$$
$$D_\xi^4 f\cdot f=2\left(f_{\xi\xi\xi\xi}f-4f_{\xi\xi\xi}f_\xi+3f_{\xi\xi}^2\right).$$

4 Solutions of TYSF equation

Case 1: Constructing $f_{11}=a_1+a_2e^{\xi_1},\xi_1=c_1\xi+c_2,m=-\frac{1}{c_1^2}$, substituting into Eq. (3.5), we collect the solution shown as follows:

$$u_{11}=\frac{2a_2c_1e^{c_1\xi+c_2}}{a_1+a_2e^{c_1\xi+c_2}},$$

where $m=-\frac{1}{c_1^2},q=-\frac{11c_1^2rs^3-12c_1^2rs^2-3p^2}{4s}$.

Constructing $f_{11}=a_1+a_2e^{-\xi_1},\xi_1=c_1\xi+c_2,m=-\frac{1}{c_1^2}$, we gather solution shown as follows:

$$u_{12}=-\frac{2a_2c_1e^{-c_1\xi-c_2}}{a_1+a_2e^{-c_1\xi-c_2}},$$

where $m=-\frac{1}{c_1^2},q=-\frac{11c_1^2rs^3-12c_1^2rs^2-3p^2}{4s}$.

The graph of solution u_{11},u_{12} are shown in Figure 1 and Figure 2.

Case 2: Similar to Case 1, constructing the activation function $f_{12}=a_1e^{-\xi_1}+a_2\cos(\xi_2)+a_3e^{\xi_1},\xi_1=b_1\xi+b_2,\xi_2=c_1\xi+c_2$, solution attained is shown as follows:

$$u_{21}=\frac{2(-a_1b_1e^{-b_1\xi-b_2}-a_2c_1\sin(c_1\xi+c_2)+a_3b_1e^{b_1\xi+b_2})}{a_1e^{-b_1\xi-b_2}+a_2\cos(c_1\xi+c_2)+a_3e^{b_1\xi+b_2}},$$

where $b_1=\frac{1}{2},c_1=\frac{Rootof(z^2+1)}{2},r=m(3p^2-4q),q=\frac{3p^2}{4}$, or $b_1=-\frac{1}{2},c_1=\frac{Rootof(z^2+1)}{2},r=m(3p^2-4q),q=\frac{3p^2}{4}$.

Using activation function $f_{12}=a_1e^{-\xi_1}+a_2\sin(\xi_2)+a_3e^{\xi_1},\xi_1=b_1\xi+b_2,\xi_2=c_1\xi+c_2$, solution is shown as follows:

$$u_{22}=\frac{2(-a_1b_1e^{-b_1\xi-b_2}-a_2c_1\cos(c_1\xi+c_2)+a_3b_1e^{b_1\xi+b_2})}{a_1e^{-b_1\xi-b_2}+a_2\sin(c_1\xi+c_2)+a_3e^{b_1\xi+b_2}},$$

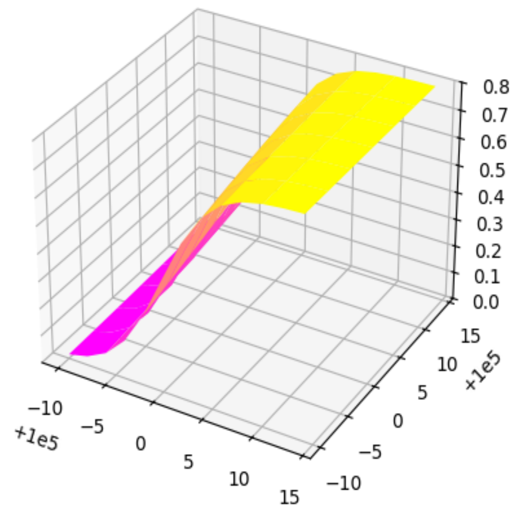

Fig. 1: Kink solution u_{11} when $p=0.1;q=0.2;r=0.3;c1=0.4;c2=0.5;a2=0.6;a1=0.7;z=0.8;t=0.1$. Source: created by the authors.

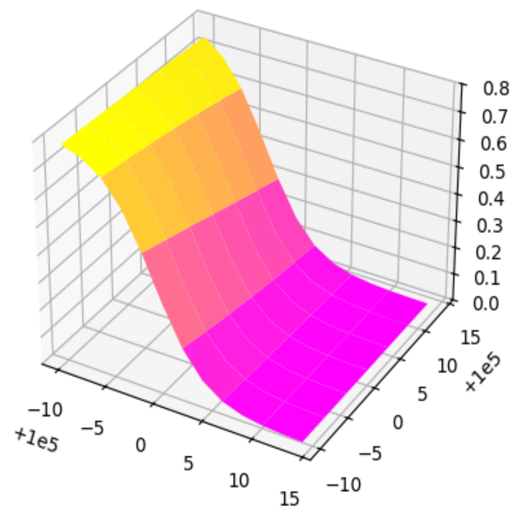

Fig. 2: Anti-kink solution u_{12} when $p=0.1;q=0.2;r=0.3;c1=0.4;c2=0.5;a2=0.6;a1=0.7;z=0.8;b1=0.1;b2=0.2;a3=0.3$. Source: created by the authors.

where $b_1=\frac{1}{2},c_1=\frac{Rootof(z^2+1)}{2},r=m(3p^2-4q),q=\frac{3p^2}{4}$, or $b_1=-\frac{1}{2},c_1=\frac{Rootof(z^2+1)}{2},r=m(3p^2-4q),q=\frac{3p^2}{4}$.

The graph of solution u_{21},u_{22} are shown in Figure 3 and Figure 4.

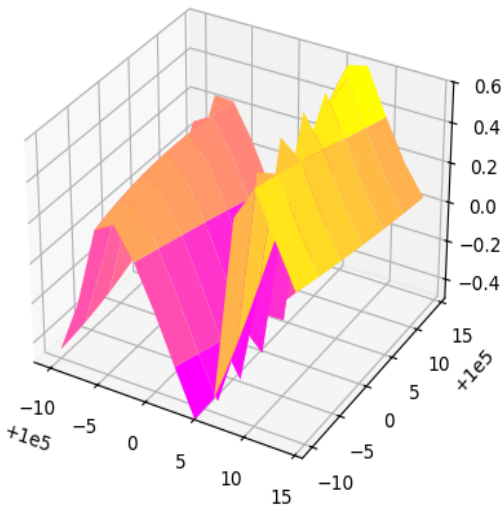

Fig. 3: Peak solution u_{21} when $p=0.1; q=0.2; r=0.3; c1=0.4; c2=0.5; a2=0.6; a1=0.7; z=0.8; b1=0.1; b2=0.2; a3=0.3$. Source: created by the authors.

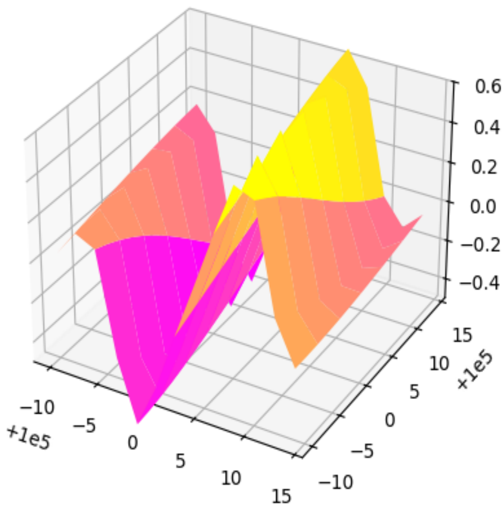

Fig. 4: Peak solution u_{22} when $p=0.1; q=0.2; r=0.3; c1=0.4; c2=0.5; a2=0.6; a1=0.7; z=0.8; b1=0.1; b2=0.2; a3=0.3$. Source: created by the authors.

Case 3: Constructing the test function $f_{31}=a_1e^{\xi_1}+a_2\cos(\xi_2), \xi_1=b_1\xi+b_2, \xi_2=c_1\xi+c_2, \xi_3=d_1\xi+d_2$, the solution is given as follows:

$$u_{31}=\frac{2a_1b_1e^{b_1\xi+b_2}-2a_2c_1\sin(c_1\xi+c_2)}{a_1e^{b_1\xi+b_2}+a_2\cos(c_1\xi+c_2)},$$

where $b_1=Rootof(z^2+1)c_1, m=\frac{1}{4c_1^2}, r=\frac{3p^2-4q}{4c_1^2}$.

Using test function $f_{31}=a_1e^{\xi_1}+a_2\sin(\xi_2), \xi_1=b_1\xi+b_2, \xi_2=c_1\xi+c_2, \xi_3=d_1\xi+d_2$, the solution is given as follows:

$$u_{32}=\frac{2a_1b_1e^{b_1\xi+b_2}-2a_2c_1\cos(c_1\xi+c_2)}{a_1e^{b_1\xi+b_2}+a_2\sin(c_1\xi+c_2)},$$

where $b_1=Rootof(z^2+1)c_1, m=\frac{1}{4c_1^2}, r=\frac{3p^2-4q}{4c_1^2}$.

The graph of solution u_{21}, u_{22} are shown in Figure 5 and Figure 6.

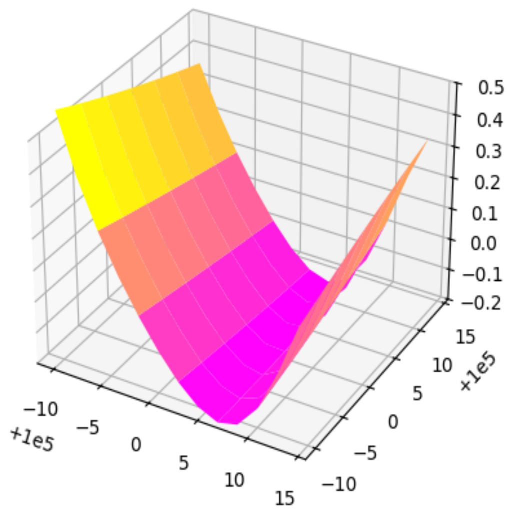

Fig. 5: V-shaped solution u_{31} when $p=0.1; q=0.2; r=0.3; c1=0.4; c2=0.5; a2=0.6; a1=0.7; z=0.8; b1=0.1; b2=0.2; a3=0.3$. Source: created by the authors.

Constructing test function $f_{41}=a_0e^{\xi_1}+a_1\sin(\xi_2)+a_2\cos(\xi_2)+a_3e^{-\xi_1}, \xi_1=b_1\xi+b_2, \xi_2=c_1\xi+c_2, b_1=Rootof(z^2+1)c_1, m=\frac{1}{4c_1^2}$, the solution is shown as follows:

$$u_{41}=\frac{\left(\begin{array}{c}2a_0b_1e^{b_1\xi+b_2}+2a_1c_1\cos(c_1\xi+c_2)\\-2a_2c_1\sin(c_1\xi+c_2)-2a_3b_1e^{-b_1\xi-b_2}\end{array}\right)}{\begin{array}{c}a_0e^{b_1\xi+b_2}+a_1\sin(c_1\xi+c_2)+a_2\cos(c_1\xi+c_2)\\+a_3e^{-b_1\xi-b_2}\end{array}},$$

where $b_1=Rootof(z^2+1)c_1, m=\frac{1}{4c_1^2}, r=\frac{3p^2-4q}{4c_1^2}$. The graph of solution u_{41} is shown in Figure 7. Constructing the function $f_{51}=a_0e^{\xi_1}(\cos(\xi_2)+a_1\cosh(\xi_1)), \xi_1=\xi+c_1, \xi_2=b_2\xi+c_2, b_2=Rootof(z^2+1), m=-\frac{1}{4}$, the solution shown as

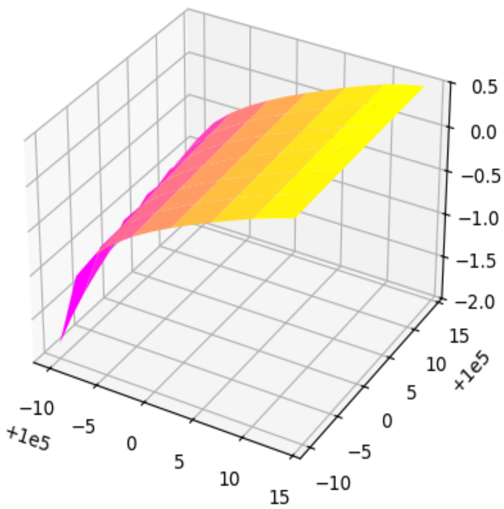

Fig. 6: V-shaped solution u_{32} when $p=0.1;q=0.2;r=0.3;c1=0.4;c2=0.5;a2=0.6;a1=0.7;z=0.8;b1=0.1;b2=0.2;a3=0.3$. Source: created by the authors.

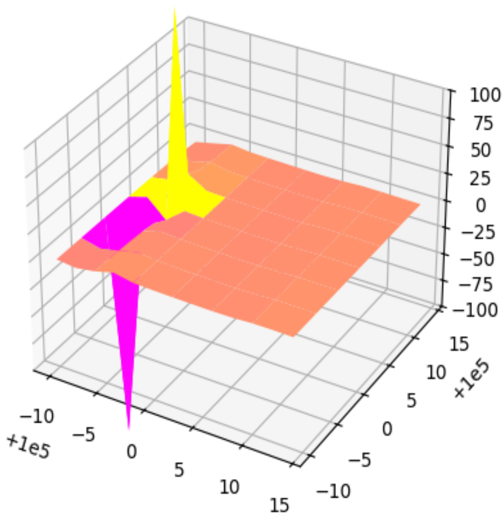

Fig. 7: Rogue solution u_{41} when $p=0.1;q=0.2;r=0.3;c1=0.4;c2=0.5;a2=0.6;a1=0.7;z=0.8;b1=0.1;b2=0.2;a3=0.3;a0=0.5$. Source: created by the authors.

follows:

$$u_{51}=\frac{\left(\begin{array}{c}2a_1\cosh(\xi+c_1)-2b_2\sin(b_2\xi+c_2)\\+2a_1\sinh(\xi+c_1)+2\cos(b_2\xi+c_2)\end{array}\right)}{\cos(b_2\xi+c_2)+a_1\cosh(\xi+c_1)},$$

where $b_2=Rootof(z^2+1),m=-\frac{1}{4},r=-\frac{3p^2}{4}+q$.

Building the test function $f_{61}=a_0+a_1e^{\xi_1+\xi_2}\sin(\xi_1),\xi_1=\xi+c_1,\xi_2=b_2\xi+c_2,b_2=Rootof(z^2+2z+2),m=1/4$, the solution is shown as follows:

$$u_{61}=\frac{2a_1e^{b_2\xi+c_1+c_2+\xi}(\sin(\xi+c_1)(b_2+1)+\cos(\xi+c_1))}{a_0+a_1e^{b_2\xi+c_1+c_2+\xi}\sin(\xi+c_1)},$$

where $b_2=Rootof(z^2+2z+2),m=\frac{1}{4},r=\frac{3p^2}{4}-q$.

The graph of solution u_{51},u_{61} are shown in Figure 8 and Figure 9.

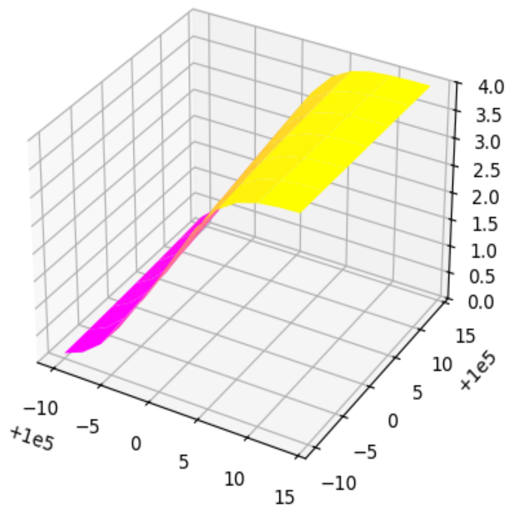

Fig. 8: Kink solution u_{51} when $p=0.1;q=0.2;r=0.3;c1=0.4;c2=0.5;a2=0.6;a1=0.7;z=0.8;b1=0.1;b2=0.2;a3=0.3;a0=0.5$. Source: created by the authors.

5 Limitations and Discussions

Although the Bilinear Neural Network Method (BNNM) demonstrates strong potential for solving the (3+1)-dimensional potential YTSF equation, some limitations remain. First, the construction of solutions relies heavily on the coefficient conditions derived from the Hirota bilinear form. These constraints may restrict the generality of the solutions and prevent the discovery of more complex wave structures. Second, while the BNNM avoids the need for large training datasets, the method still requires careful selection of test functions and parameter tuning, which can limit automation and scalability for broader classes of nonlinear PDEs. Another limitation concerns computational efficiency when extending the approach to higher-dimensional or fractional-order systems. The algebraic complexity increases rapidly, which may affect the feasibility

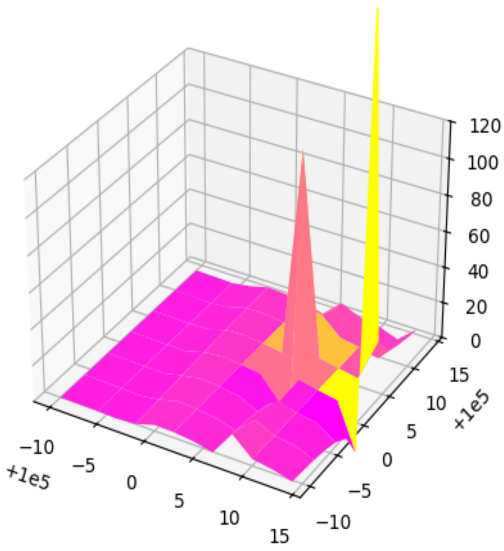

Fig. 9: Lump solution u_{61} when $p = 0.1; q = 0.2; r = 0.3; c1 = 0.4; c2 = 0.5; a2 = 0.6; a1 = 0.7; z = 0.8; b1 = 0.1; b2 = 0.2; a3 = 0.3; a0 = 0.5$. Source: created by the authors.

of deriving fully explicit closed-form solutions. Moreover, the current work focuses primarily on idealized mathematical models; further validation in applied physical contexts, such as fluid dynamics or plasma physics, remains necessary to confirm the physical significance of the obtained solutions. Despite these limitations, the results highlight the value of combining integrable systems theory with neural network techniques. The BNNM provides an effective compromise between analytical rigor and computational flexibility, offering new insights into the dynamics of nonlinear evolution equations. Future research should explore adaptive extensions of the method, hybrid frameworks with symbolic computation, and applications to experimental data-driven models, which could further enhance its practicality and relevance.

6 Conclusion

In this study, the (3+1)-dimensional potential YuTodaSasaFukuyama (YTSF) equation was analyzed through the Bilinear Neural Network Method (BNNM). By integrating Hirotas bilinear formalism with neural network modeling, several exact solution classes were obtained, including kink-type solutions, lump solutions, rogue solutions, peak solutions and V-shaped solutions. The findings confirm that BNNM offers a systematic and efficient framework for solving high-dimensional nonlinear partial differential equations without requiring extensive training data. Compared with traditional perturbation or numerical discretization approaches, the method maintains mathematical rigor while providing greater flexibility in capturing diverse nonlinear wave phenomena. These results broaden the understanding of wave dynamics modeled by the YTSF equation and highlight promising applications in fluid dynamics, plasma physics, and related scientific fields. Future work may extend this framework to fractional-order systems, nonlocal integrable equations, and higher-dimensional models, further advancing its role in nonlinear science and computational mathematics.

Acknowledgment:
We sincerely appreciate the financial research support of the Posts and Telecommunications Institute of Technology in Ho Chi Minh City, Viet Nam, and for providing the necessary resources, a conducive research environment that contributed significantly to the success of this study.

References:

[1] Deng, G.-F., Gao, Y.-T., Su, J.-J., & Ding, C.-C. (2019). Multi-breather wave solutions for a generalized (3+1)-dimensional Yu-Toda-Sasa-Fukuyama equation in a two-layer liquid. Applied Mathematics Letters, 98, 177-183. `https://doi.org/10.1016/j.aml.2019.05.037`

[2] Huang, L., Manafian, J., Singh, G., Nisar, K. S., & Nasution, M. K. M. (2021). New lump and interaction soliton, N-soliton solutions and the LSP for the (3 + 1)-D potential-YTSF-like equation. Results in Physics, 29, 104713. `https://doi.org/10.1016/j.rinp.2021.104713`

[3] Zhu, Q., & Qi, J. (2022). On the Exact Solutions of Nonlinear Potential Yu-Toda-Sasa-Fukuyama Equation by Different Methods. Discrete Dynamics in Nature and Society, 2022(1), 2179375. `https://doi.org/10.1155/2022/2179375`

[4] Plaatjie, K., & Khalique, C. M. (2021). On the solutions and conservation laws of the YuTodaSasaFukuyama equation of plasma physics. Results in Physics, 29, 104706. `https://doi.org/10.1016/j.rinp.2021.104706`

[5] Adeyemo, O. D. (2025). Real-World Applications of Analytic Travelling Wave Solutions of a (3+1)-Dimensional HirotaSatsumaIto-Like System Via Polynomial Complete Discriminant System and Elementary Integral Technique. International Journal of

Applied and Computational Mathematics, 11(2), 23. https://doi.org/10.1007/s40819-025-01836-7

[6] Chen, H., Xu, Z., & Dai, Z. (2014). Rogue Wave for the (3+1)-Dimensional Yu–Toda–Sasa–Fukuyama Equation. Abstract and Applied Analysis, 2014, 1, 378167. https://doi.org/10.1155/2014/378167

[7] Yin, H.-M., Tian, B., Chai, J., Wu, X.-Y., & Sun, W.-R. (2016). Solitons and bilinear Bäcklund transformations for a (3 + 1) -dimensional Yu-Toda-Sasa-Fukuyama equation in a liquid or lattice. Applied Mathematics Letters, 58, 178-183. https://doi.org/10.1016/j.aml.2016.02.011

[8] Khan, K., & Akbar, M. A. (2014). Solitons and Periodic Wave Solutions of The (3+1)-dimensional Potential YuTodaSasa Fukuyama Equation. Physical Review, 4, 1, 181-197. https://journalpsij.com/index.php/PSIJ/article/view/150 [Access Date: 01/01/2026]

[9] Tuan, N. M., & Meesad, P. (2025). New solutions of sixth-order Benney-Luke equation using bilinear neural network method. Zeitschrift Fur Angewandte Mathematik Und Physik, 76, 133. https://doi.org/10.1007/s00033-025-02516-8

[10] Usman, T., & Ullah, M. S. (2025). Analytical solutions and chaotic insights into the Hirota-Maccari system. Scientific Reports, 15, 43540. https://doi.org/10.1038/s41598-025-27419-6

Contribution of Individual Authors to the Creation of a Scientific Article (Ghostwriting Policy)

Nguyen Minh Tuan: Conceptualization, data curation, investigation, methodology, software, validation, visualization, writing-original draft and writing-review and editing; Chau Van Van, Nguyen Hong Son, Huynh Trong Thua, Le Ha Thanh: software, visualization, validation, supervisor, writing-review and editing.

Sources of Funding for Research Presented in a Scientific Article or Scientific Article Itself

No funding was received for conducting this study.

Conflicts of Interest

The authors have no conflicts of interest to declare that are relevant to the content of this article.

APPENDIX

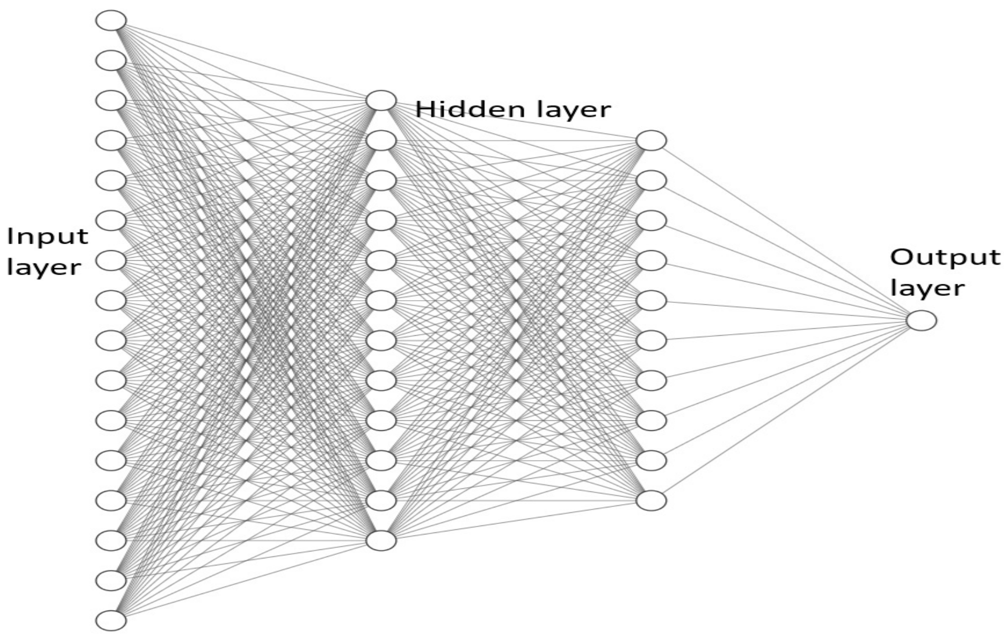

Fig. 1: Bilinear neural network model.
Source: created by the authors.